Yi Liu[1]
Weizhong Qian[1]
Qiang Zhang[1]
Guoqing Ning[1]
Guohua Luo[1]
Yao Wang[1]
Dezheng Wang[1]
Fei Wei[1]

[1] Beijing Key Laboratory of Green Chemical Reaction Engineering and Technology, Tsinghua University, Beijing, P. R. China.

Research Article

Synthesis of High-Quality, Double-Walled Carbon Nanotubes in a Fluidized Bed Reactor

Double-walled carbon nanotubes (DWCNTs) were synthesized in a packed bed reactor (PBR) and a fluidized bed reactor (FBR) by cracking CH_4 on a Fe/MgO catalyst. It is observed that the dominant carbon product changes drastically from DWCNTs to multi-walled CNTs along the axial direction of PBR. The studies indicated that the high concentration of H_2 from the high conversion of CH_4 causes the quick reduction and sintering of the iron catalyst and inhibits the nucleation of DWCNTs. Based on these results, the batch or continuous feeding mode of small amounts of catalyst was adopted in a FBR to maintain a high space velocity of CH_4 and to inhibit the negative effect of excess H_2. Finally, a DWCNT product with a specific surface area of 950 m^2/g and a purity of 98 %, was obtained.

Keywords: Carbon nanotubes, Catalysts, Chemical vapor deposition, Fluidized beds, Hydrogen effect

Received: June 16, 2008; *revised:* September 05, 2008; *accepted:* September 24, 2008

DOI: 10.1002/ceat.200800298

1 Introduction

Double-walled carbon nanotubes (DWCNTs) with excellent mechanical, electrical and chemical properties find potential applications in polymer composites, field emissions and battery materials [1, 2]. However, to date, their mass production remains a challenge, whether using laser-ablation, arc-discharge or chemical vapor deposition (CVD) methods. Compared with the two former methods, CVD has potential advantages in producing DWCNTs, single-walled carbon nanotubes (SWCNTs) or their mixtures with high selectivity at a small scale of milligrams to grams [3–11]. However, the mass production of DWCNTs is hardly reported. Though some reports have discussed the mass production of SWCNTs [12–14], they may be different for DWCNTs. Recent study suggests that the wall number control of SWCNTs is relatively tough as compared to that of multi-walled carbon nanotubes (MWCNTs) [10, 11]. In this case, the higher metal loading on the catalyst for the DWCNT growth than that for the SWCNT growth makes it more difficult to avoid sintering than for the latter, when operated in the same high temperature range. Moreover, to synthesize bulk DWCNTs, it is necessary to control the concentration of the carbon source and the gas velocity [14], the thermal stability of the catalyst [10, 11], the contact time of the catalyst with the carbon source [12], as well as the agglomerate structure of the carbon products [14] so that these are similar to those in the synthesis of MWCNTs [15–19].

In this report, it is attempted to understand which effect is crucial to the scaled up synthesis of DWCNTs, using the CH_4–Fe/MgO catalyst CVD system. For the first time, significantly different carbon products were obtained along the axial direction of a packed bed reactor (PBR) holding the same catalyst and operated at the same temperature. The evidence from the gas analysis in different parts, as well as the calculations, both support the view that the concentration change in H_2 causes the sintering of the metal particles and inhibits the nucleation of DWCNTs. Based on this finding, a relative comprehensive study is presented on the effect of H_2 and two methods are proposed to control the space velocity of CH_4 in a fluidized bed reactor (FBR), to control the concentration of H_2 and its negative effect. These methods allow the relatively large-scale production of DWCNTs with a high purity in a FBR.

2 Experimental

2.1 Synthesis of DWCNTs

The PBR reactor composed of quartz was 6 mm in diameter. The Fe/MgO catalyst with 3 mol.-% Fe loading was prepared by an impregnation method [10] (labeled as C1). After calcination at 600 °C for 2 h in air, 0.2 g catalyst was put into PBR and was quickly heated to 800 °C in an Ar flow. Then a mixed gas (47.5 % CH_4 as the carbon source, 2.5 % H_2 and 50 % Ar

Correspondence: Prof. W. Z. Qian (qianwz@mail.tsinghua.edu.cn), Beijing Key Laboratory of Green Chemical Reaction Engineering and Technology, Department of Chemical Engineering, Tsinghua University, Beijing, 100084, P. R. China.

© 2009 WILEY-VCH Verlag GmbH & Co. KGaA, Weinheim

as the carrier gas, all gases are of 99.99 % purity) flux of 20 mL/min was fed into the PBR to grow DWCNTs for 15 min to ensure all catalysts were deactivated.

For the synthesis of DWCNTs in a FBR (i.d. 50 mm, shown in Fig. 1), ca. 20 g catalyst was fed after the FBR was heated to 850 °C. Then the flux of mixed gas (25 % CH_4 as the carbon source and 75 % Ar as the carrier gas) of 4 L min^{-1} was fed into the FBR to grow DWCNTs for 30 min. To test the feeding mode of the catalyst, ca. 0.2 g of catalyst was fed into the FBR in batches at different intervals, e.g., 1 min or 15 s, and CH_4 was cut off 5 min later, after a total of 20 g of catalyst was fed in and to ensure all catalysts were deactivated.

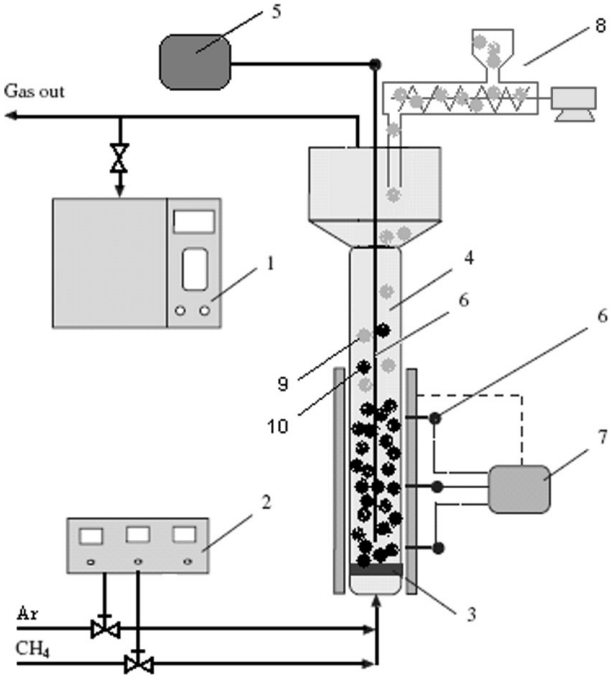

Figure 1. Schematic of the FBR system for DWCNT synthesis. (1) Gas chromatogram, (2) Mass flow controller, (3) Gas distributor, (4) FBR, (5) Temperature recorder, (6) Thermocouple, (7) Furnace temperature controller, (8) Screw feeder, (9) Fresh catalyst, and (10) As-grown product.

2.2 Characterization of Carbon Products

The height of the catalyst bed containing the carbon product in PBR is ca. 22 mm. The carbon products were sampled at different positions along the axial direction of the PBR. Samples were characterized by scanning electron microscope (SEM, JSM7401F, 3.0 kV), transmission electron microscope (TEM, JEOL2010F, 120.0 kV), Raman microscope (RM2000, 633 nm), thermogravimetric analysis (TGA, TA2050) and single point BET specific surface area (SSA) measurement. The contents of amorphous carbon and CNTs on the catalyst were determined by TGA based on their different burning temperatures, e.g., amorphous carbon burnt before 400 °C while CNTs burnt between 400 and 650 °C (burning temperature of MWCNTs is higher than that of DWCNTs).

Since SSA for the pure DWCNTs, amorphous carbon/MWCNTs, and catalyst is 600–1000, 100–200, and 50 m^2/g [20–23], respectively, one can qualitatively use SSA to evaluate the quality of carbon product under the effect of H_2. Apparently, a higher SSA of the gross sample means a higher content of DWCNT in the sample.

3 Results and Discussion

3.1 Synthesis of DWCNTs in PBR

Fig. 2 shows SEM images of carbon products at different axial positions of the PBR. The dominant product near the entrance is uniform DWCNT bundles with a uniform diameter of 10–20 nm, a length of several tens of micrometers, and a high growth density, Fig. 2a). In comparison, the density of DWCNT bundles is low and there are many MWCNTs of 20–50 nm in diameter in the sample at 11 mm from the entrance, Fig. 2b). The content of DWCNTs is ca. 50 %. Moreover, in the sample at a distance of 22 mm from the gas entrance, the DWCNTs content decreased to 33 %. Meanwhile, the fibers became relatively short and are unable to form bundles, Fig. 2c).

Furthermore, Raman scattering was used to characterize samples present in large amounts, Fig. 2d). Alhough all products have peaks present at 100–250 cm^{-1}, demonstrating the existence of DWCNTs, the intensity ratio of the *D* band (~ 1324 cm^{-1}) to *G* band (~ 1590 cm^{-1}), i.e., I_D/I_G ratio, varies with the samples in different positions. In summary, the I_D/I_G ratio increases monotonously from 0.099 (near the entrance) to 0.168 (near the exit), indicating the gradually increasing content of carbon impurities in the product along the axial direction of the PBR [7–11, 13, 15, 16].

Meanwhile, the SSA of the mixed sample gradually decreased from 170 m^2/g at the entrance to 65 m^2/g at the exit, Fig. 2e). Since the content of amorphous carbon is almost constant in all samples determined by TGA, this means the CNT content decreases gradually along the axial direction of the PBR, Fig. 2f). The SSA of pure CNT in samples at different positions is determined according to the SSA of the gross product and the contents of CNTs and amorphous carbon, Fig. 2e). This is 680–800 m^2/g at the entrance, 200–600 m^2/g in the middle section and < 200 m^2/g at the exit, respectively. Moreover, the burning temperature of CNTs in TGA increased from 556 to 571 °C along the axial direction, also indicating the increasing content of MWCNTs. Considering the significant difference in SSA of the different carbon products mentioned above and the evidence from SEM, TEM, TGA and Raman taken together, it can be concluded that the dominant carbon products gradually change from the DWCNT bundle at the entrance to the MWCNTs at the exit. This is the first report of morphology and structural changes of the CNTs in different positions of the reactor when using the same catalyst.

© 2009 WILEY-VCH Verlag GmbH & Co. KGaA, Weinheim

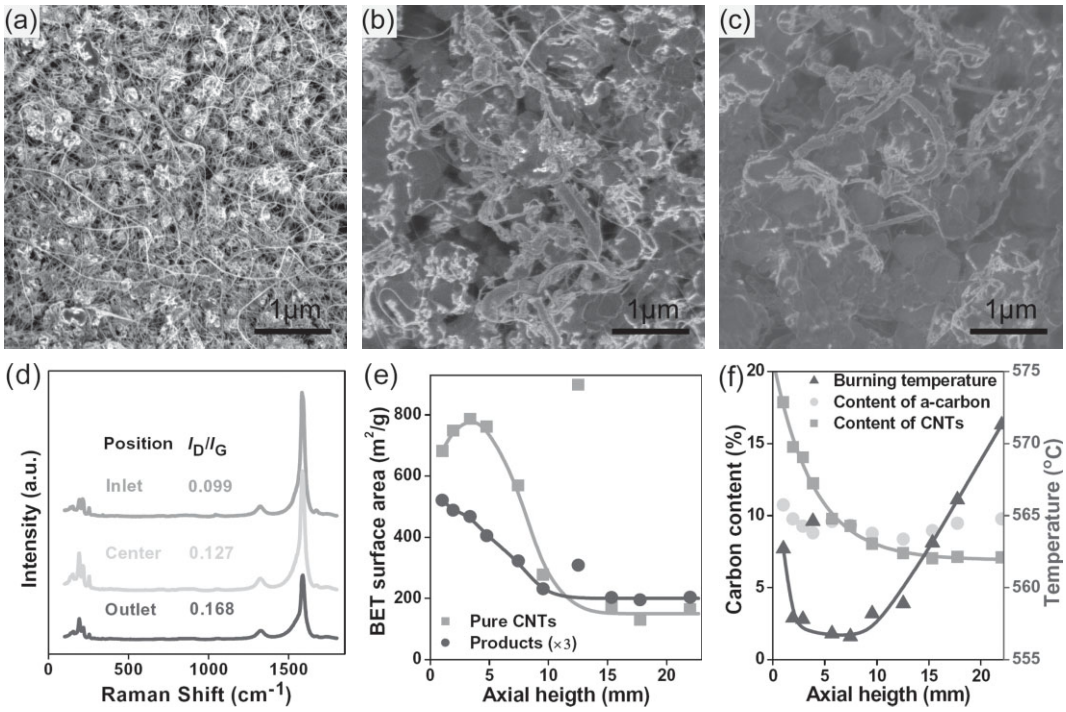

Figure 2. Characterization of carbon products as-grown at different positions of the PBR. (a) DWCNTs at entrance (0 mm), (b) DWCNTs and carbon filaments (11 mm), (c) DWCNTs and carbon filaments (22 mm), (d) Raman spectra of carbon products at different positions, (e) Contents of CNT and amorphous carbon on the catalyst, and (f) SSA of gross samples and calculated values for carbon along the axial position of the PBR.

3.2 Nucleation of DWCNT on a Catalyst and Sintering of Metal Catalyst

The nucleation and growth of CNTs can be considered as self-assembly of carbon atoms into tubes on metal nanoparticles (NPs) [24]. The diameter of the CNTs depends on the size of metal NPs [25–27]. Usually, SWCNTs/DWCNTs and MWCNTs grow on NPs smaller than 3–5 nm and 5–100 nm in size, respectively. Thus, the change of product from DWCNTs to MWCNTs reflects the gradual size increase of the metal NPs on the catalyst in different positions of the PBR, which is confirmed by the TEM observations, Fig. 3. The average diameter of the Fe NPs (4, 6 and 8.5 nm from the entrance to the exit) becomes larger along the axial position of the PBR and the distribution gets broader. Since the catalyst remains static in the reactor and is of the same size before the reaction, such changes indicate the sintering of metal NPs during the reaction.

It is worth noting that the fresh catalyst is iron oxide on a MgO support. The sintering of iron oxide at high temperatures is not serious due to its strong interaction with MgO [28].When the iron oxide turns into Fe after reduction by H_2 or CH_4, the interaction between Fe and MgO is weak due to the higher surface energy of Fe than MgO [29, 30]. Fe atoms will then aggregate together to form Fe NPs.

The nucleation of DWCNTs and the sintering of Fe NPs can be considered as two parallel competitive reactions. If sufficient carbon deposits on the appropriate sized metal catalyst, carbon will precipitate onto the surface of Fe NPs. The surface energy will be lowered due to the lower surface force of graphite, i.e., 0.1 J/m^2, compared to that of liquid Fe, i.e., 1.4–1.8 J/m^2, and the sintering of NPs will be inhibited. DWCNTs will also nucleate well on NPs of appreciable size. However, if the carbon supply is insufficient, the lack of the protection of graphite causes the rapid sintering of Fe NPs, which consequently produces large diameter MWCNTs. The scheme is shown in Fig. 4.

The concentration distributions of H_2 and CH_4 along the axial direction of the PBR were estimated and are shown in Fig. 5. At the entrance, the concentration of CH_4 was highest, and the content of H_2 was lowest. With the gradual conversion of CH_4, the concentration of H_2 increased significantly, which accelerated the sintering of Fe NPs accordingly [29]. In addition, in a condition rich in H_2, the carbon supply is insufficient and the DWCNT nucleation will be restrained [31]. In detail, the DWCNT nucleation is restricted when the conversion of CH_4 is over 77.2 %. However, the DWCNT growth, if already nucleated, continues until the conversion of CH_4 is 94.3 %. Since the kinetic constant of this reaction is 70 s^{-1} (as discussed in Sect. 3.5), the conversion of CH_4 will be above 77.2 % and the calculated concentration of H_2 is higher than 56 % at a distance of 1.4 mm away from the entrance of the PBR for the fresh catalyst, Fig. 5a). In this case, the DWCNT cannot nucleate on the catalyst far away from the entrance

© 2009 WILEY-VCH Verlag GmbH & Co. KGaA, Weinheim

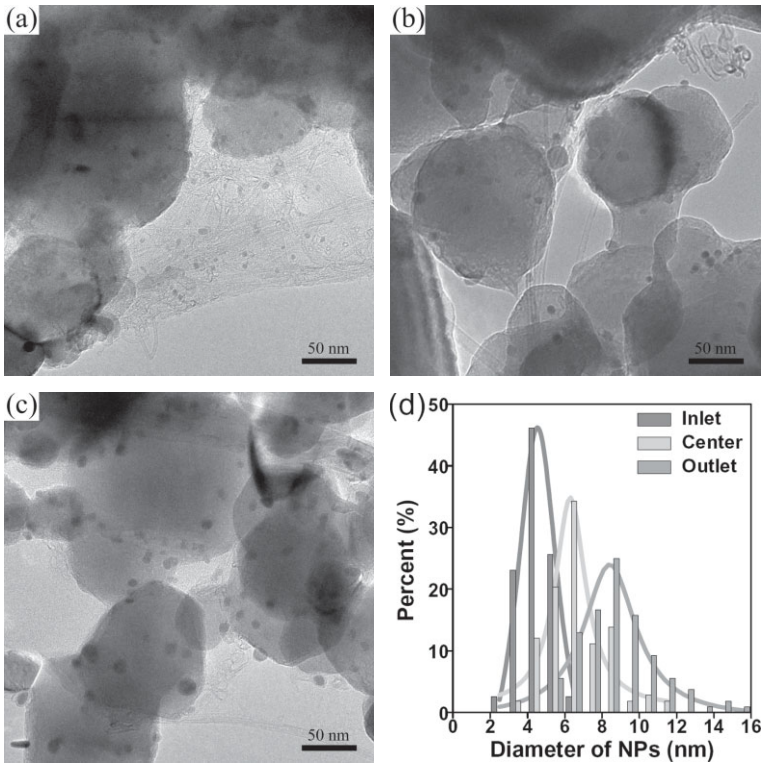

Figure 3. Sintering of Fe NPs along the axial position of PBR. (a) Entrance (0 mm), (b) Center (11 mm), (c) Exit (22 mm), and (d) Diameter distribution of Fe NPs.

unless the front catalyst is deactivated first. The sintering times of Fe NPs in a high concentration of H_2 (> 60 %), roughly estimated, are 5 min and 9 min in the middle part and exit of the reactor, respectively, Fig. 5b), assuming the stepwise deactivation of the catalyst in the PBR. Fe NPs sinter seriously in such a long growth time, and consequently, result in large diameter MWCNTs. Since the metal loading is the same for all catalysts, the formation of large Fe NPs naturally decreases the amount of small Fe NPs for the synthesis of DWCNT/SWCNT. Therefore, the growth density of DWCNTs decreases significantly and the SSA of the carbon product decreases gradually, as discussed previously.

3.3 Tailoring the Nucleation of DWCNTs by Space Velocity and Partial Pressure of CH_4

The above findings indicate the complexity in scaling up the production of DWCNTs using large amounts of catalyst and in reactors of large sizes. Apparently, such a negative effect of H_2 directly depends on the deep conversion of CH_4 in certain thicknesses of catalyst bed or the amount of catalyst present. The concentration of H_2 can be tailored by varying the amount of catalyst and the flow rate of CH_4. Fig. 6a) demonstrates that the use of small amounts of catalyst, while keeping the flow rate of CH_4 constant, is effective for increasing the SSA of the gross product from 100 to 270 m^2/g. The situation is the same for catalysts prepared by different methods, i.e., co-precipitation and hydrothermal treatment, labeled as C2. Similar results are achieved by increasing the flow rate of CH_4, Fig. 6b). Reducing the partial pressure of CH_4 by adding Ar is also effective to reduce the concentration of H_2, similar to the effect demonstrated by Nagy et al. [32], and is effective to increase the SSA of mixed catalyst and CNT samples, Fig. 6c).

When the space velocity of CH_4 is 0.75 L/g min, the partial pressure of CH_4 plays an important role in the SSA of the product. However, it is not significant as the space velocity decreases, e.g., to 0.25 L/g min, at partial pressure values of 0.1. On the other hand, the SSA is low even at a space velocity of 3 L/g min when the partial pressure of CH_4 is higher than 0.8. It should be noted that the extrapolation of the SSA of gross product by different partial pressures of CH_4 will give a value of 310 m^2/g (corresponding to a space velocity of ca. 10 L/g min^{-1}), which may be the up-limit for this catalyst considering the confined levels for growth of DWCNTs in porous catalysts [33].

When using a Fe/MgO catalyst with 1 % Fe to prepare SWCNTs, a similar H_2 effect was observed and a similar improvement was obtained by tailoring the space velocity or the partial pressure of CH_4. The H_2 effect is general for the growth

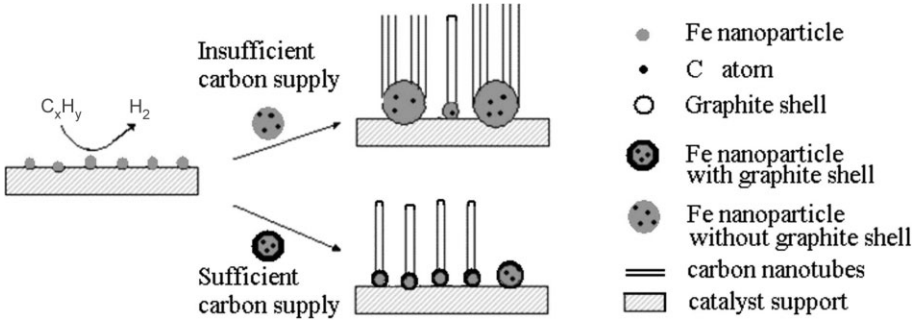

Figure 4. Scheme of the nucleation of DWCNT and sintering of Fe NPs.

© 2009 WILEY-VCH Verlag GmbH & Co. KGaA, Weinheim

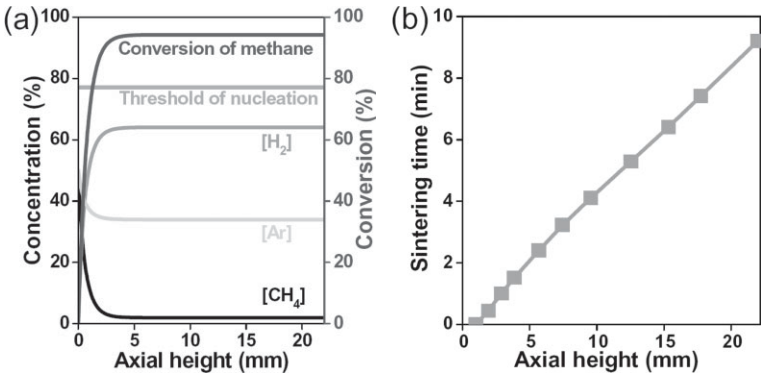

Figure 5. (a) Conversion of CH_4 and concentration of gases along the axial position of the PBR, and (b) Sintering time of catalyst in high concentration of H_2 (> 60 %).

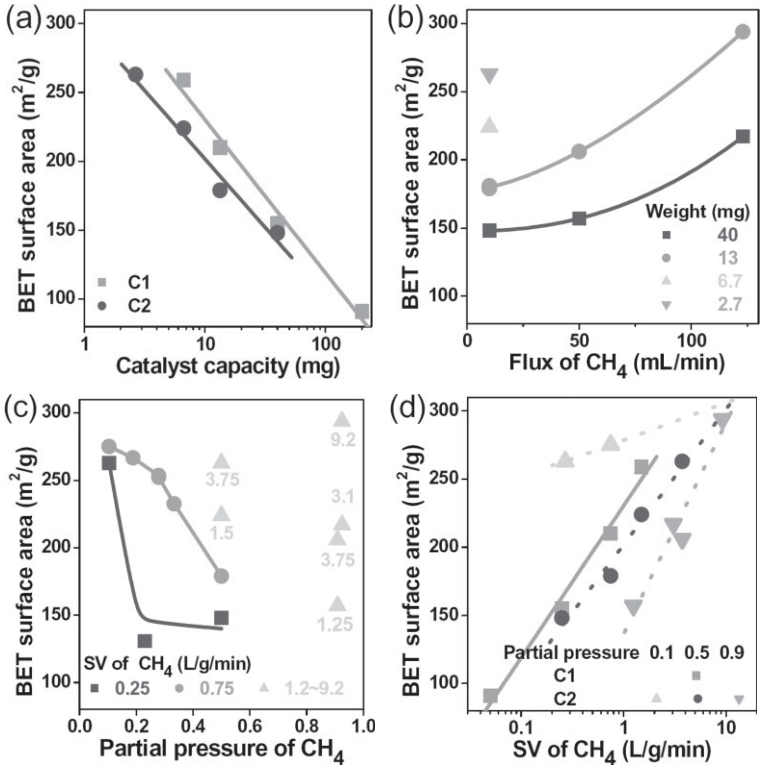

Figure 6. Effects of efforts to control the BET surface area of samples containing CNTs and catalyst. (a) Effect of catalyst weight on the SSA of samples, (b) Effect of CH_4 flux on the SSA of samples, (c) Effect of partial pressure of CH_4 on the SSA of samples, (d) Effect of space velocity of CH_4 on the SSA of samples. (Note: Catalyst used for Figs. 6b) and 6c) is C2.)

of SWCNTs or DWCNTs, similar to the report of Nagy et al. [32]. The authors reported that the gases contact insufficiently with the catalyst in the horizontal flow of the PBR [32], because the catalyst is only sprayed onto the bottom surface of the quartz tube. Hence, the negative effect of H_2 in their work is not as serious as reported here.

3.4 Synthesis of DWCNTs in a FBR

Since the synthesis of DWCNTs is a quickly deactivated process with a characteristic time of ca. 1–3 min and the size of catalyst particles is usually tens of micrometers, the FBR has advantages over the PBR in the continuous and mass production of DWCNTs, e.g., with a continuous feeding catalyst in or transporting products out at any desired time [15, 16].

The product in a FBR has a higher SSA (~ 120 m^2/g) than that (98 m^2/g) in a PBR, indicating the better synthesis of DWCNTs in the FBR. However, the selectivity of DWCNTs was still worse due to the low space velocity of CH_4. The dominant carbon product was flexable MWCNTs of 10–20 nm diameter when the catalyst was fed in a one-off manner, labeled as P1 in Figs. 7a) and 7b).

Since the sintering of Fe NPs is time-dependent, two approaches are adopted here to increase the space velocity of CH_4 for the DWCNT growth. Firstly, on increasing the absolute flow rate of CH_4 and the space velocity to 4 L g^{-1} min^{-1}, both high quality DWCNTs and high conversion of CH_4 are obtained due to the short residence time of catalyst and the fast carbon deposition on the reduced catalyst, Fig. 5c). However, this method seems difficult to scale up because the correspondingly high gas velocity influences the stable fluidization of the catalyst and CNTs with a low bulk density in the FBR. Another approach is to reduce the load of catalyst and to increase the space velocity of CH_4 accordingly. In actual fact, when an inert medium, e.g., deactivated products, was preloaded in a FBR to maintain efficient fluidization, and the catalyst was fed in batches, e.g., 0.2 g of catalyst per min was fed per batch, the space velocity of CH_4 can be high up to 5 L g^{-1} min^{-1}, due to the low weight ratio of the catalyst, and is two orders of magnitude larger than that for a once-off catalyst feeding. Such high space velocity is suitable for the nucleation of a high density of DWCNTs. Abundant DWCNT products, free of any MWCNTs or onion-like carbon, are obtained, labeled as P3 in Figs. 7c) and 7d).

The effect of feeding intervals on the morphology of product was also studied. On keeping the same space velocity, the feeding of 0.2 g catalyst at intervals of 15 s (labeled as P2) actually achieved worse results. The content of DWCNTs decreased, Figs. 7e) and 7f), probably due to the incomplete deactivation of pre-added catalyst and the high concentration of H_2, as well as the insufficient growth of DWCNTs in the short time intervals. From this point of view, the batch feeding mode of the catalyst in small amounts is better than the continuous feeding of a catalyst in small amounts. Even if the latter approach is adopted, the amount of the catalyst should be strictly controlled.

© 2009 WILEY-VCH Verlag GmbH & Co. KGaA, Weinheim

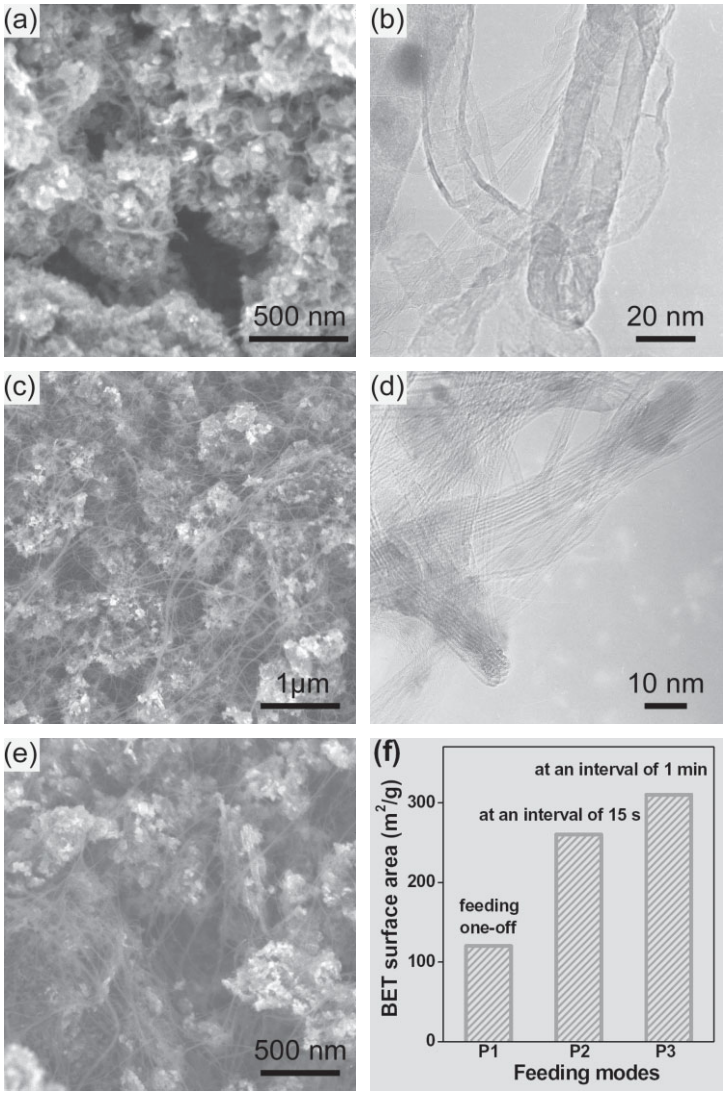

Figure 7. (a, c, e) SEM, (b, d) TEM morphologies and (f) BET specific surface areas of products with different feed rates: (a, b) one-off feeding, (c, d) feeding in batches at an interval of 1 min, and (e) feeding in batches at an interval of 15 s.

The SSA of the gross products is shown in Fig. 7f). A high SSA product was found for a low feeding rate of the catalyst, consistent with the SEM and TEM observations, Fig. 7. As an example, the SSA and carbon content (measured by TGA) for P3 are 317 m^2/g and 33.8 %, respectively. Thus, the calculated SSA of the DWCNTs is 840 m^2/g. Moreover, after purification by HCl acid to remove the catalyst support, the purity of the carbon product is 98 wt % and its SSA is 950 m^2/g, Fig. 8. The measurement of ca. 150 CNTs showed that the purified products contained 90 % DWCNTs of diameter 1.4–4.0 nm, and ca. 10 % SWCNTs of diameter 1–1.5 nm. No other carbon impurities were found except for several tri-walled CNTs. The logarithmic diameter distribution of the products fits well with the diameter centered at 2.0 nm (with a correlated coefficient larger than 0.99). The synthesis of DWCNTs with high selectivity is attributed to the effective control of the low concentration of H_2 in the FBR with a high space velocity of CH_4.

3.5 Kinetics in the PBR and FBR

In addition, the kinetic constant was estimated for CH_4 decomposition, which can be described by a first-order dependence on CH_4 [34][1)]:

$$r = kP_{CH_4} \quad (1)$$

For the integral reactor, one obtains Eq. (2):

$$c = c_0 e^{-kt} \quad (2)$$

The conversion of methane is 58 % for a 6.7 mg catalyst bed. The packed density of catalyst is 0.35 kg/L, and the fluxes of CH_4 and Ar are both 10 mL min^{-1}. The dynamic rate constant, k, was calculated as 70 s^{-1} at 800 °C, and as 92 s^{-1} at 850 °C by considering the changeable gas volume and reversible reaction, both of which are close to the value of 60 s^{-1} calculated by Eq. (2). They are both far larger than the value of 3.84 s^{-1} calculated by Ago's group, where a quarter of the Fe content of the present work was used [35].

For the current DWCNT synthesis in the FBR, the calculated contact time of the catalyst with the gases is 2.2 ms, assuming the same catalyst stack state as in the PBR. The average conversion of CH_4 is 18.1 %, and therefore, the average calculated kinetic constant is 106 s^{-1}, assuming the CSTR gas flow in the FBR. Considering the quick deactivation of catalyst, i.e., usually with the activity down by 30 % in 1 min, the kinetic constant in the FBR within 1 min will be much larger than 106 s^{-1}, which is far larger than the value of 92 s^{-1} for the PBR. Apparently, the lower partial pressure of CH_4 in the entrance and lower concentration of H_2 in the exhaust gas due to the back-mixing in FBR, are both favorable for the nucleation and growth of DWCNTs. Thus, it can be concluded that the decomposition of CH_4 is more efficient in the FBR than in the PBR, similar to the results for MWCNT production [36]. These results are favorable for the scaling up of production of DWCNTs at low cost.

4 Conclusions

In a scaled-up production of DWCNTs in a CH_4-Fe/MgO CVD system, H_2 has a negative effect on the stability of the catalyst, and consequently, the selectivity of DWCNTs, along the axial direction of a PBR. Decreasing the concentration of H_2 by increasing the space velocity of CH_4, using several meth-

1) List of symbols at the end of the paper.

© 2009 WILEY-VCH Verlag GmbH & Co. KGaA, Weinheim

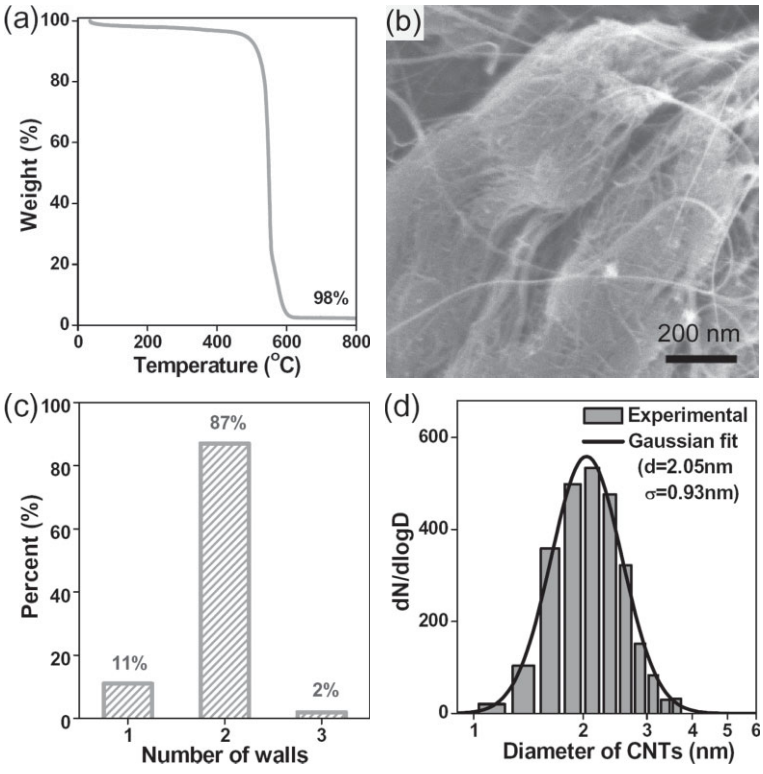

Figure 8. (a) TGA, (b) SEM, (c) Wall, and (d) Diameter distribution of a purified sample of P3.

ods, is effective for increasing the selectivity of DWCNTs. A very high space velocity of CH_4, which can be achieved by feeding fresh catalyst in small amounts (in continuous or batch mode) in a FBR is effective to make DWCNTs of high purity and selectivity.

Acknowledgements

The work was supported by the FANEDD (Grant No. 200548), NSFC program or key program (Grant Nos. 20606020, 20736004, and 20736007), China National program (Grant No. 2006CB932702). The authors are grateful to Prof. D. Z. Wang for helpful discussions.

Symbols used

c	[mol/L]	concentration of reactant
c_0	[mol/L]	initial concentration of reactant
k	[1/s]	kinetics constant
P	[kPa]	pressure of reactant
r	[kPa/s]	rate of reaction

References

[1] R. H. Baughman, A. A. Zakhidov, W. A. Heer, *Science* **2002**, *297 (5582)*, 787.
[2] P. M. Ajayan, *Chem. Rev.* **1999**, *99 (7)*, 1787.
[3] M. Su, B. Zheng, J. Liu, *Chem. Phys. Lett.* **2000**, *322 (5)*, 321.
[4] J. F. Colomer et al., *Chem. Phys. Lett.* **2000**, *317 (1–2)*, 83.
[5] Q. W. Li et al., *J. Mater. Chem.* **2002**, *12 (4)*, 1179.
[6] H. Yan, Q. W. Li, J. Zhang, Z. F. Liu, *Carbon* **2002**, *40 (14)*, 2693.
[7] S. C. Lyu et al., *Chem. Mater.* **2003**, *15 (20)*, 3951.
[8] E. Flahaut et al., *J. Mater. Chem.* **2004**, *14 (4)*, 646.
[9] G. Q. Ning, F. Wei, G. H. Luo, Y. Jin, *Carbon* **2005**, *43 (7)*, 1439.
[10] G. Q. Ning et al., *J. Phys. Chem. C* **2007**, *111 (5)*, 1969.
[11] Q. Wen et al., *Chem. Mater.* **2007**, *19 (6)*, 1226.
[12] Y. L. Li et al., *Chem. Mater.* **2004**, *16 (26)*, 5637.
[13] E. Mora, T. Tokune, A. R. Harutyunyan, *Carbon* **2007**, *45 (5)*, 971.
[14] Q. F. Zhang et al., *New Carbon Mater.* **2006**, *21 (4)*, 349.
[15] Y. Wang et al., *Chem. Phys. Lett.* **2002**, *364 (5–6)*, 568.
[16] W. Z. Qian et al., *AIChE J.* **2003**, *49 (3)*, 619.
[17] M. Corrias et al., *Chem. Eng. Sci.* **2003**, *58 (19)*, 4475.
[18] Y. Hao et al., *Carbon* **2003**, *41 (14)*, 2855.
[19] H. Yu et al., *AIChE J.* **2006**, *52 (12)*, 4110.
[20] B. C. Liu, M. Z Qu, Z. L. Yu, *Chin. Chem. Lett.* **2001**, *12 (12)*, 1135.
[21] G. Pastorelli, R. Canziani, L. Pedrazzi, A. Rozzi, *Water Sci. Technol.* **1999**, *40 (4–5)*, 169.
[22] C. Kern, A. Jess, *Chem. Eng. Sci.* **2005**, *60 (15)*, 4249.
[23] F. X. Li, Y. Wang, D. Z. Wang, F. Wei, *Carbon* **2004**, *42 (12–13)*, 2375.
[24] H. J. Dai et al., *Chem. Phys. Lett.* **1996**, *260 (3–4)*, 471.
[25] Y. M. Li et al., *J. Phys. Chem. B* **2001**, *105 (46)*, 11424.
[26] C. L. Cheung, A. Kurtz, H. Park, C. M. Lieber, *J. Phys. Chem. B* **2002**, *106 (10)*, 2429.
[27] J. H. Hafner et al., *Chem. Phys. Lett.* **1998**, *296 (1–2)*, 195.
[28] H. Ago, K. Nakamura, N. Uehara, M. Tsuji, *J. Phys. Chem. B* **2004**, *108 (49)*, 18908.
[29] H. Kanzow, A. Ding, *Phys. Rev. B: Condens. Matter Mater. Phys.* **1999**, *60 (15)*, 11180.
[30] R. Seidel et al., *J. Phys. Chem. B* **2006**, *108 (6)*, 1888.
[31] L. M. Wagg et al., *J. Phys. Chem. B* **2005**, *109 (20)*, 10435.
[32] J. B. Nagy et al., *J. Nanosci. Nanotechnol.* **2004**, *4 (4)*, 325.
[33] Y. Liu et al., *Carbon* **2008**, *46 (14)*, 1860.
[34] J. M. Wei, E. Iglesia, *J. Phys. Chem. B* **2004**, *108 (13)*, 4094.
[35] H. Ago et al., *Carbon* **2006**, *44 (14)*, 2912.
[36] S. W. Liu, Y. D. Li, *J. Chem. Ind. Eng.* **2007**, *58 (1)*, 102.

© 2009 WILEY-VCH Verlag GmbH & Co. KGaA, Weinheim